ELSEVIER

Coordination Chemistry Reviews 144 (1995)
347–368

COORDINATION CHEMISTRY REVIEWS

Molecular aspects of iron uptake and storage in ferritin

Pamela M. Proulx-Curry, N. Dennis Chasteen*

Department of Chemistry, University of New Hampshire, Durham, NH 03824, USA

Received 17 December 1994; revised 27 February 1995

Contents

Abstract

The iron storage protein ferritin is composed of 24 subunits of two types, H and L, which assemble to form a hollow protein shell capable of encapsulating up to 4500 Fe atoms in the form of a hydrous ferric oxide mineral core. Iron is oxidized for incorporation into the mineralized core by either a protein enzymatic mechanism involving a putative dimeric Fe ferroxidase site on the H chain subunit or a mineral surface mechanism. The net stoichiometric reactions for the two kinetic pathways are given by the following equations:

$$2Fe^{2+} + O_2 + 4H_2O \rightarrow 2FeOOH_{core} + H_2O_2 + 4H^+$$

$$4Fe^{2+} + O_2 + 6H_2O \rightarrow 4FeOOH_{core} + 8H^+$$

The L chain subunit appears to be involved mostly in mineralization of the core but modulates the ferroxidase activity of the H chain subunit as well. A reaction mechanism in which Fe(II) oxidation occurs in one electron steps accounts for the observed kinetics. Several reaction intermediates have been identified using UV–visible, electron paramagnetic resonance and Mössbauer spectroscopies but their roles in the mechanism of iron deposition in the protein remain to be determined.

* Corresponding author.

SSDI 0010-8545(95)01148-X

Keywords: Ferritin; Iron uptake; Iron storage

List of abbreviations

Ec-BFR	heme containing bacterioferritin from *Escherichia coli*
Ec-FTN	non-heme containing bacterioferritin from *E. coli*
HLF	human liver ferritin
HoSF	horse spleen ferritin
HuHF	human H chain ferritin
HuLF	human L chain ferritin

1. Introduction

Iron, the fourth most abundant element in the Earth's crust, is essential to all life. The redox potential range of Fe(II/III) is wide (−500 to +300 mV) depending on its coordination. In living organisms iron is involved in such diverse processes as oxygen transport, nitrogen fixation, electron transfer reactions, and photosynthesis [1,2]. Indeed, life as we know it could not have evolved without this essential and ubiquitous transition metal.

The iron storage protein ferritin protects cells from the potentially toxic effects of free iron by sequestering iron in a mineralized form within the protein for later use by the cell in the synthesis of heme. Our knowledge of ferritin has increased rapidly in recent years because of the availability of recombinant proteins, site-directed variants, high resolution crystal structures and assays for the oxidation reactions occurring during core formation. The reader is referred to the many excellent reviews which cover studies performed earlier [2–11]. Here we review the literature in the past five years focusing on the molecular aspects of iron binding, oxidation, and incorporation into the mineral core.

2. Structure of ferritin

Ferritins are present in the cells of vertebrates, invertebrates, plants, and bacteria. Amino acid sequences are known for ferritins from a number of mammals, red cells of the bullfrog *Raba catesbeinna* and of the chicken *Gallus*, the parasite *Schistosoma mansoni*, the freshwater snail *Lymnea stagnalis*, soybeans and pea seeds, and the bacteria *Azotobacter vinelandii* and *Nitrobacter winogradskyi* [1,3,4,7]. Two types of ferritin have been isolated from the bacterium *Escherichia coli*, a heme-containing bacterioferritin (Ec-BFR) [12] and a non-heme ferritin-like protein (Ec-FTN) [13]. While the primary and three-dimensional structure of mammalian ferritin has been reviewed in detail elsewhere [2–4,7,8,11,14], a brief summary is presented here.

Mammalian ferritins are composed of two polypeptide chains, H (heavy) and L

(light), with apparent molecular weights of 21 000 and 19 000 respectively, based on small differences in their relative mobilities on sodium dodecylsulfate–polyacrylamide gel electrophoresis [15]. The relative amounts of each chain present in ferritin are tissue specific. While the similarity between species of a specific chain is high (80% identity between human, rat and horse L chains, and 90% identity between human, rat, and chicken H chains), the H and L chains themselves are only about 50% homologous [4]. Soybean and pea seed ferritins are more similar to the H chains of mammals and chickens than to the L chains. The heme-containing bacterioferritins, on the contrary, exhibit little similarity to animal ferritins (21% identity with human and chicken H chains, and 18%–19% with human and horse L chains), and even less (14% identity) to the ferritin-like protein (Ec-FTN) isolated from *E. coli* [3,4,7].

The three-dimensional structures of all ferritins are essentially the same with the 24 subunits assembled in the form of a hollow protein shell [3] (Fig. 1). The H and L chain subunits have similar conformations with the atoms of the peptide backbone superimposable upon each other within about 0.1 nm [3,4]. Each subunit consists of five α-helices, A–E. Four of them (A–D) form antiparallel helix pairs A–B and C–D which are connected by a loop L (Fig. 2). In the subunit dimers these loops interact to form a β-sheet within the dimer (Fig. 3). 12 dimers combine to form a hollow, 24-mer spherical structure with 4:3:2 cubic symmetry. The β-sheets formed by the interactions of the L loops lie at the external surface of the protein shell. The *N*-terminal sequences of the subunits project towards the outer surface of the shell. At the *C*-terminal end a fifth helix, E, extends at an angle of approximately 60° from the A–D helix bundle. A short chain of amino acid residues extends from the end of the E helix into the cavity of the protein shell at an angle almost perpendicular to the inner surface. The association of two subunits into a dimer forms a groove with 2-fold symmetry on the inner surface of the shell. Except for a number of narrow channels that lead to the protein's inner cavity, the protein shell is close packed because of many intersubunit interactions [2,4,11,14,16].

The ferritin molecule in most species contains six hydrophobic channels about 0.4–0.5 nm wide which lie along the 4-fold symmetry axes and are lined with 12 leucine residues [3,11,17,18a]. In the recently crystallized bullfrog L chain ferritin, however, the side chains are tightly packed at this axis and create a gap about 0.15 nm wide rather than a channel [18b]. Eight funnel-shaped hydrophilic channels, with average diameters of about 0.6 nm in the human H chain and about 0.7 nm in the bullfrog L chain ferritin, lie along the 3-fold axes [18b]. Three glutamic acid and three aspartic acid residues near the middle of this channel are highly conserved in mammals and plants, but less so in invertebrates and bacteria [3,11,17,18a]. Three histidine, six serine, and three cysteine residues line the outer edge of the hydrophilic channels [18a].

Up to 4500 iron atoms, or about 30% (by weight) Fe, can be stored within the protein shell [19]. The iron is deposited as a ferric hydrous oxide phosphate core with a structure similar to that of the geological mineral ferrihydrite [20a]. The iron oxide phase is microcrystalline with a unit cell based on a four-layer repeat of h.c.p. oxygen atoms (Fig. 4) [11]. There is a wide variation in the phosphate content of the cores of various ferritins with Fe:P ratios ranging from 21:1 in human thalassemia

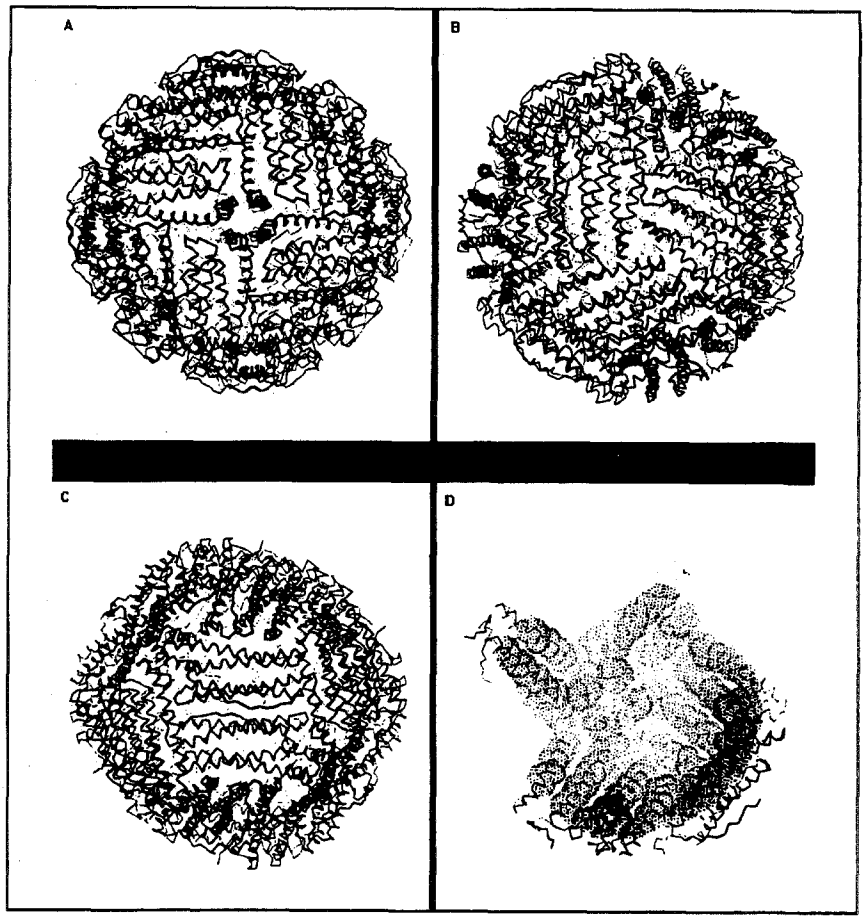

Fig. 1. Computer graphics drawings depicting features of the horse spleen apoferritin structure: molecule viewed down the (a) 4-, (b) 3- (c) 2-fold axes; (d) part of the inside of the apoferritin shell showing the inner ends of the four E helices. Adapted with permission from Ref. [8].

spleen ferritin [20b] to almost 1:1 in *Pseudomonas aeruginosa* bacterioferritin [19]. Likewise, core crystallinity covers a broad spectrum from single-domain crystals resembling ferrihydrite ($5Fe_2O_3 \cdot 9H_2O$) in some human ferritins to cores of limited crystallinity in ferritins from the limpet *Patella vulgata* to cores with no crystallinity in ferritins from the bacteria *Ps. aeruginosa* [21].

3. The ferroxidase site and other metal binding sites

Iron(II) oxidation is a necessary step for the incorporation of iron into the ferritin core. Oxidation may either be catalyzed at specific ferroxidase sites on the protein shell [22] or occur directly on the surface of the growing mineralized core [23]. In

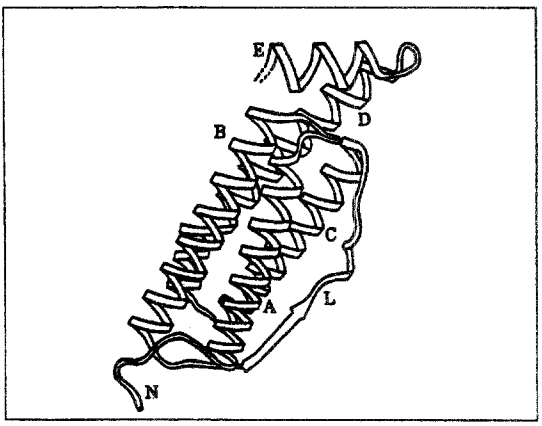

Fig. 2. Ribbon diagram of the α-carbon backbone of a horse spleen apoferritin subunit. The main body of the subunit is a bundle of four long helices, A, B, C, and D, with a short helix, E, lying at an acute angle to the bundle axis. The *N*-terminus, *N*, lies at the other end of the subunit to E. The loop, L, joins helices B and C and together with its 2-fold related counterpart, L′, forms a section of antiparallel β-sheet within the dimer. The final two residues in the *C*-terminal tail are not included in this diagram. Reprinted with permission from Ref. [11].

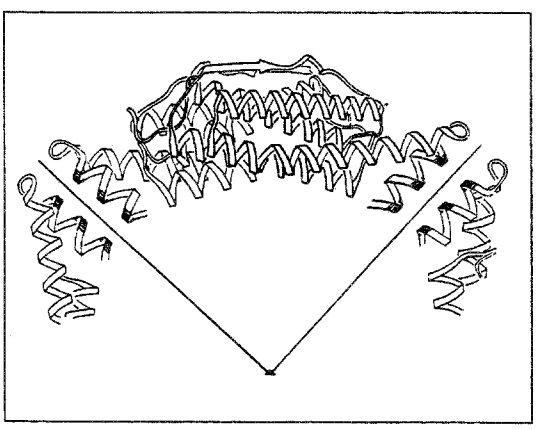

Fig. 3. Ribbon diagram of the horse spleen apoferritin dimer and parts of two other subunits. The hydrophobic face of helix E is shaded. Reprinted with permission from Ref. [11].

recent years the location and structure of the ferroxidase sites have been established with reasonable certainty. The non-heme-containing ferritin isolated from *E. coli* bacteria (Ec-FTN) has recently been crystallized in the absence of metal ions and its three-dimensional structure determined [24]. Three iron binding sites (sites A, B, and C) are seen on the protein (Fig. 5) which become occupied with iron atoms when the metal free crystals are soaked in a solution of ferrous ammonium sulfate, $Fe(NH_4)_2(SO_4)_2$, in the presence of atmospheric oxygen. These three sites lie within 0.7 nm of each other with the A and B sites, which constitute the postulated ferroxi-

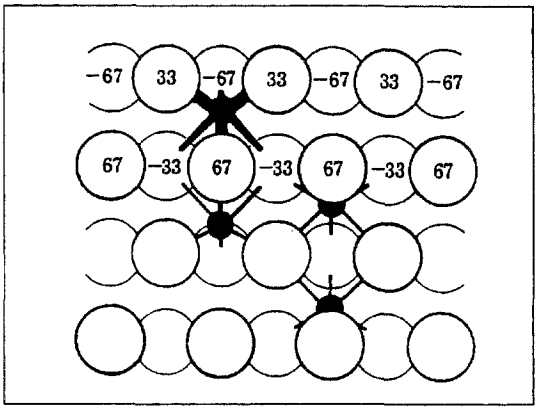

Fig. 4. The Towe and Bradley model for "ferrihydrite" showing four oxygen (○) layers with iron (●) atoms octahedrally coordinated. Reprinted with permission from Ref. [11].

dase center, only about 0.38 nm apart. The ligands at site A are Glu 27, Glu 62, and His 65. Those at site B are Glu 62 (which acts as a bridging ligand), Glu 107, and Glu 144 (see Fig. 5). The residue Gln 141 may also be linked to iron bound to sites A and B through water, although it is not close enough to bind directly to either iron [24]. Fe(A) (iron bound to site A) and Fe(B) (iron bound at site B) are present on the same subunit and may be joined through a μ-oxo (or OH^- or H_2O) bridge, although no bridging atom is seen in the structure at its current resolution [24].

Unlike sites A and B, the third iron binding site, site C, differs from any binding site observed in HuHF, HoSF or rat liver ferritin [4,16]. The site consists of four ligands: Glu 61, Glu 140, Glu 143, and Glu 144. Only Glu 61 is conserved among all known ferritins except Ec-BFR, although Glu 140 is present in HuHF. Glu 144 is found only in Ec-FTN, the glutamate being replaced by alanine in the mammalian H chain and leucine in the L chain [3,24].

Prior to the direct observation of the dimeric iron binding site in Ec-FTN discussed above [24], a great deal of information about the ferroxidase site had been obtained through site-directed mutagenesis experiments with the human protein [25–31] in conjunction with X-ray crystallography [16,24,27]. The amino acid sequence change Lys 86 → Gln in recombinant human H chain ferritin (HuHF) permitted crystallization of this ferritin [16]. An electron density map calculated at 0.25 nm resolution for Tb(III) soaked crystals revealed three Tb(III) binding sites: A, B, and C. Both sites A and B are located within the subunit about 0.7–0.8 nm from the inner surface of the shell and 1.0–1.2 nm from the outside within the four α-helix bundle [16]. Narrow channels about 0.1 nm in width lead to the sites from both the outside and the inside of the protein. In L chain subunits these channels are blocked by a salt bridge [16]. Three amino acid ligands, Glu 27, Glu 62, and His 65 (human H chain numbering) are present at site A of the human protein [16]. The Tb(III) atom at site A has tetrahedral coordination, the fourth position apparently occupied by a water molecule. The second Tb(III), at site B, is coordinated by the ligands Glu 61,

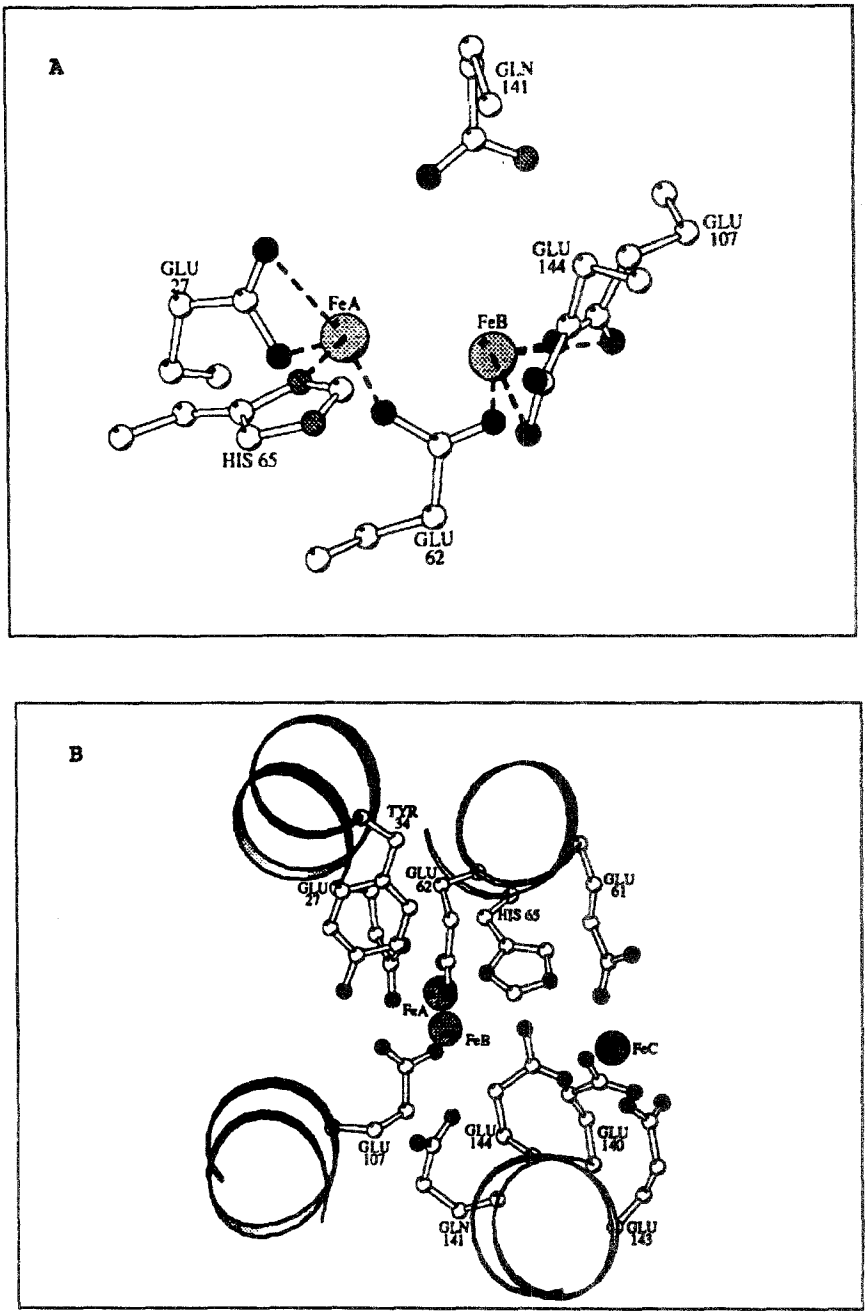

Fig. 5. (A) Computer generated model of the A–B diiron site of *E. coli* non-heme-containing ferritin (Ec-FTN). (B) Model of the A, B, and C iron sites in Ec-FTN viewed down the axis of the four-helix bundle. Outside surface of the shell on the left, inside on the right. Reprinted with permission from Ref. [24].

Glu 62, and Glu 107 with Glu 61 appearing to alternate between two positions. Sites A and B are quite similar to those observed in Ec-FTN [24] mentioned above and the modeled Fe(III) sites reported by Treffry and coworkers [29]. Indeed, when the Ec-FTN cystals are soaked in $TbCl_3$, Tb(III) ions bind at the A and B sites of that ferritin [24].

The third Tb(III) binding site on the HuHF, site C, is observed on the inside surface of the molecule bound to the residues Glu 61 and Glu 64 [16]. Unlike the residues at site A, which are conserved in all known H chain subunits but are absent from L chain [16], those of binding site C are conserved in the L chain subunit as well as the H chain [16], and perhaps play a role in core nucleation. On the basis of these observations and the effect of site-directed mutagenesis on iron oxidation [16,26,27,29,30,32] discussed later, the sites inside the four α-helix bundles were correctly predicted to be the most likely location of the ferroxidase center [27] as later confirmed by the structure of Ec-FTN [24].

Further evidence that the ferroxidase site resides within the H subunit was obtained from Mössbauer spectroscopic studies [26,29,32]. Many Fe(III) clusters, relative to other iron species, are observed in solutions of horse spleen apoferritin (apo-HoSF) only 40 s after loading the protein with Fe(II) in the presence of oxygen, while very few Fe(III) clusters and many Fe(II) ions are found in the protein-free solution, thus establishing the catalytic activity of the apoprotein toward iron oxidation [32]. Rates of iron oxidation in proteins with putative ferroxidase residues (Glu 62, His 65) of HuHF mutated to the amino acids of the L form are much less than those obtained from proteins with intact sites [16,27,29,32], and even less than the rate in protein free solutions [29,32]. One minute after loading with Fe(II) the dimer species are the dominant form in HuHF with intact ferroxidase sites [26,32]. The major species in a solution of HuHF with mutated ferroxidase site residues, however, is Fe(II) with a very small amount of Fe(III) clusters, and no evidence of Fe(III) dimers or monomers [26]. In HoSF the dimer is the minor species which is consistent with the small number of H chain subunits found in HoSF [32]. Variants in which the 3-fold channels (Asp 131, Glu 134), the 4-fold channels (Leu 169, His 173) or the putative nucleation sites (Glu 61, Glu 64, Glu 67) had been modified still generate dimers, providing further evidence that the ferroxidase site is located in the H subunit at the A–B dimer site [26,30,32].

The effects of mutating residues on the *C*-terminus, which forms the hydrophobic channels, and around the L loop were also examined. Those mutations which do not decrease the protein's thermostability, or prevent it from assembling, have no effect on iron uptake [33]. Mutagenesis studies do implicate the 3-fold channels in iron uptake (Fig. 6) [17,33].

Taken together the above data indicate that iron uptake rates are faster with more Fe(III) dimers being produced in H chain-containing proteins with intact ferroxidase centers than in L chain homopolymers or variants with modified ferroxidase site ligands. These results are consistent with the hypothesis that the ferroxidase site is the dimeric site recently observed by X-ray crystallography on the H chain subunit of Ec-FTN [24].

In addition to Fe(II) and Fe(III), a variety of other metal ions bind to ferritin

Fig. 6. Hydrophilic pathway between the 3-fold channels and the ferroxidase center of the human H chain ferritin. Reprinted with permission from Ref. [17].

and apoferritin [16,34,35]. The binding properties of many of these metals were exploited in early studies in an attempt to gain information about binding sites on ferritin and the kinetics of iron uptake [16,28,34–43]. Metals such as Cd(II), Tb(III), and VO(IV) appear to share some binding sites with iron and so have been used to probe structure and binding stoichiometry [16,38–40,42]. Others such as Ru(II), Cd(II), Co(II), Tb(III), Cu(II), and Zn(II) inhibit iron oxidation in the protein [28,34–37], with Zn(II) being the most effective inhibitor [36]. Metal binding at or near the 3-fold hydrophilic channels has been implicated by a number of studies [34,35,38,42]. Because many of these metals may bind at several sites on the protein with different affinities, interpretation of data obtained from metal binding studies has not always been straightforward. Site-directed mutagenesis studies have helped

to overcome this problem and are responsible for much of the insight into the function of ferritin gained over the last five years.

4. Ferroxidase kinetics

Two models of Fe(II) oxidation in ferritin were proposed over a decade ago, the protein catalysis model and the crystal growth model [22,23]. Detailed analysis of the kinetics of iron oxidation was not possible at that time because of a lack of knowledge of the stoichiometric equations for the reactions involved and the need for a direct assay of iron oxidation. The traditional method of following color changes in the protein solution to monitor iron oxidation does not provide the type of data needed for detailed kinetics studies, especially of the early phase of the reaction. Moreover, it is known that color changes from the accumulation of Fe(II) in ferritin can occur even in the absence of iron oxidation [44].

Several measurements of the stoichiometry of iron oxidation have been made over the years with results ranging from 1.5 to 4.0 Fe(II) oxidized per dioxygen reduced, depending on the conditions of the experiment and the methods employed for measuring consumption of Fe(II) and oxygen [45–47]. More recent experiments using ^{16}O mass spectrometry and ^{57}Fe Mössbauer spectroscopy [48] showed that, when small increments of Fe(II) (24 Fe(II) per protein) were added to horse spleen apoferritin, the oxidation stoichiometry was clearly 2 Fe(II) per dioxygen as in Eq. (1). When larger increments (up to 960 Fe(II) per protein) were added, the stoichiometry increased to 4 Fe(II) per dioxygen (Eq. (2)), corresponding to a change from a protein ferroxidase catalytic mechanism to a mineral surface dominated mechanism of iron oxidation [48]. The variability and fractional values of previously reported stoichiometries of iron oxidation [45–47] can be understood on this basis. Two protons are released for each Fe(II) oxidized in accord with Eqs. (1) and (2) [48].

$$2Fe^{2+} + O_2 + 4H_2O \rightarrow 2FeOOH_{core} + H_2O_2 + 4H^+ \quad (1)$$

$$4Fe^{2+} + O_2 + 6H_2O \rightarrow 4FeOOH_{core} + 8H^+ \quad (2)$$

Measurements using electrode oximetry have permitted the kinetics of iron oxidation to be followed directly throughout the reaction from the amount of dioxygen consumed as a function of time. Horse spleen apoferritin was shown to accelerate markedly the rates of Fe(II) oxidation and oxygen consumption relative to buffer alone [37]. Saturation kinetics with respect to both the Fe(II) and dioxygen concentrations and first-order kinetics with respect to protein concentration were observed, indicating that the reaction takes place by an enzyme-catalyzed mechanism. Ferritin is unlike other enzymes, however, in that the product of the reaction, namely Fe(III), is stored within the protein itself. The apparent kinetic parameters for the enzyme reaction of three ferritins studied to date are summarized in Table 1 [37].

A similar study using electrode oximetry to measure iron oxidation reactions in solutions of human liver ferritin (HLF), H chain and L chain homopolymers, and a

Table 1
Kinetic parameters for HuHF[a], HLF[a], and HoSF[b]

	HuHF	HLF	HoSF
K_{m,O_2} (μM)	6 ± 2	60 ± 12	140 ± 30
$K_{m,Fe}$ (μM)	80 ± 10	50 ± 10	350 ± 10
k_{cat} (min^{-1})	201 ± 14	31.2 ± 0.6	80.0 ± 3.3
$K_{I,Zn}$ (μM)	74 ± 10		67 ± 11[c]
$Fe^{2+}:O_2$	2.1 ± 0.1	$< 2.7 \pm 0.1$	2.0 ± 0.2[d]
E_a (kJ mol^{-1})	26.4 ± 0.1	67.3 ± 0.5	36.6 ± 1.3
$\Delta H^{\ddagger}$ (kJ mol^{-1})	23.9 ± 0.1	64.8 ± 0.5	34.2 ± 1.3
$\Delta S^{\ddagger}$ (J mol^{-1} K^{-1})	-136.0 ± 0.4	-11.0 ± 1.6	-108 ± 5

[a] Conditions: 0.1 M NaCl, 50 mM Mops, pH 7.05, 20 °C. The composition of HLF was 4% H and 96% L subunits.
[b] HoSF was composed of 16% H and 84% L subunits. The data listed for HoSF were from Ref. [38].
[c] K_I for competitive inhibition at Zn^{2+}:protein ≥ 6.
[d] From Ref. [48]. Reprinted with permission from Ref. [28].

number of variants was also conducted [28]. From the total amount of dioxygen consumed during Fe(II) oxidation, apparent Fe(II):dioxygen stoichiometries of 2.1 ± 0.1 and 2.7 ± 0.1 were obtained for HuHF and human liver ferritin (HLF) respectively. The results were consistent with the oxidation reaction given by Eq. (1) [28]. The higher value of 2.7 Fe(II) per dioxygen for HLF, which consists of 4% H chain and 96% L chain, is a consequence of the slow rate of Fe(II) oxidation in this protein during which time some O_2 is regenerated from the disproportionation of the hydrogen peroxide produced (Eq. (3)); also some iron(II) autoxidation occurs on the surface of the ferritin core, a reaction with an Fe(II):dioxygen stoichiometry of 4.0 (Eq. (2)) [28].

$$2H_2O_2 \rightarrow O_2 + 2H_2O \tag{3}$$

From measurements on a number of variants and the wild-type protein, it was observed that those with intact H chain ferroxidase centers gave higher oxidation rates than L chain homopolymers or variants with altered ferroxidase sites (Fig. 7) [28]. Variants with altered nucleation sites, but intact ferroxidase sites, gave rates almost equal to those of wild type H homopolymers. Variants with both altered ferroxidase and nucleation sites failed to take up Fe(II) significantly. As with HoSF, saturation kinetics with respect to both Fe(II) and dioxygen concentrations was also observed for HLF and HuHF (see Table 1) [28].

Iron oxidation rates increase with increasing H chain content in the proteins. The order is reversed, however, when the results are expressed on a per H chain subunit basis (Table 2) [28]. Some cooperativity appears to exist between the two subunits, with the L chain enhancing the ferroxidase activity of the H chain, perhaps by facilitating iron turnover since the L chain appears to be more efficient that the H chain at initiating core formation [49,50]. The L chain possesses a greater negative

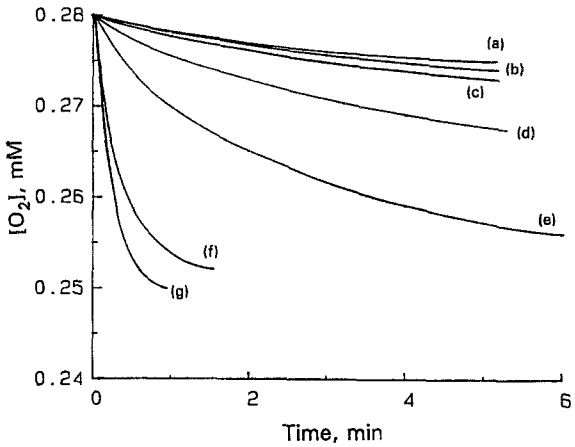

Fig. 7. Oxygen consumption vs. time for the oxidation of Fe(II) in buffer (curve a), ferroxidase and nucleation site variant, S1 (D42A, E61A, E62K, E64A, H65G, E67A, K86Q) (curve b), HuLf (curve c), ferroxidase site variant 222 (E62K, H65G, K86Q) (curve d), HLF (curve e), nucleation site variant A2 (E61A, E64A, E67A) (curve f), and HuHF (curve g). Conditions: [apoferritin] = 2.08 μM and $[Fe^{2+}]_0$ = 67 μM, in 0.1 M NaCl and 50 mM Mops buffer, pH 7.05, 20 °C. Reprinted with permission from Ref. [28].

Table 2
Comparison of k_{cat} values for HuHF[a], HoSF[b], and HLF[a]

	HuHF	HoSF	HLF
H subunit (%)	100	16	4
L subunit (%)	—	84	96
k_{cat} (min^{-1})	201	80	31
k_{cat}/(H subunit) (min^{-1} $subunit^{-1}$)	8.4	21	31

[a] HuHF and HLF data from Ref. [28].
[b] HoSF data from Ref. [38].

charge density on the inner surface of the shell which may assist in this process [49,50].

The enzyme-catalyzed reaction mechanism given by Eqs. (4)–(7) [37] explains the observed oxygen uptake kinetics according to a dimeric ferroxidase site model, where P represents the protein ferroxidase site:
first Fe(II) binding,

$$P + Fe^{2+} \underset{k_{-1}}{\overset{k_1}{\rightleftharpoons}} Fe^{2+} \cdot P \tag{4}$$

dioxygen binding,

$$Fe^{2+} \cdot P + O_2 \underset{k_{-2}}{\overset{k_2}{\rightleftharpoons}} Fe^{2+}(O_2) \cdot P \tag{5}$$

first Fe(II) oxidation,

$$Fe^{2+}(O_2)\cdot P \xrightarrow{k_3} Fe^{3+}(O_2^-)\cdot P \tag{6}$$

second Fe(II) binding–oxidation,

$$Fe^{3+}(O_2^-)\cdot P + Fe^{2+} \xrightarrow{k_4} Fe^{3+}(O_2^{2-})Fe^{3+}\cdot P \tag{7}$$

$$\xrightarrow{k_5,\,H_2O} Fe^{3+}(O^{2-})Fe^{3+} + H_2O_2$$

In this mechanism the superoxide remains bound to the first Fe(III) oxidized, accounting for the inability of earlier electron paramagnetic resonance (EPR) studies to observe O_2^- [48,51]. The second Fe(II) binds and is oxidized to form either a peroxo-bridged or a terminally bound peroxo group which ultimately leads to the formation of the Fe(III) dimer observed by Mössbauer spectroscopy [32,52,53] with hydrogen peroxide being the final product of dioxygen reduction. In this mechanism, iron(II) oxidation occurs in one-electron steps, accounting for the observed first-order kinetics in Fe(II) at low Fe(II) concentrations [37]. Under conditions of low increments of added iron (below 50 Fe per protein), the presence of a pre-existing core affects the rate of iron oxidation very little because the reaction occurs primarily via the protein-catalyzed pathway (Fig. 8). At high increments of added iron (above 50 Fe per protein) where the ferroxidase sites become kinetically saturated, autoxidation at the core surface begins to affect the observed rate (see Fig. 8) [37]. Thus

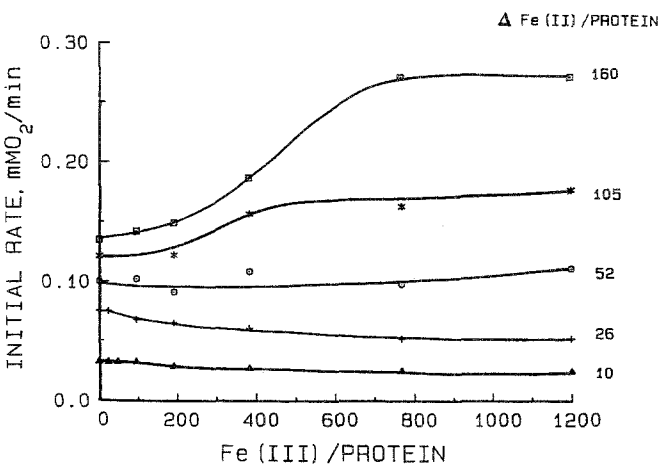

Fig. 8. Dependence of the initial rate of oxygen consumption on the increment of iron(II) added and on the amount of iron already present in horse spleen ferritin. Increments of iron(II), ΔFe(II), were added to samples of ferritin containing from 0 to 1200 Fe(III) per protein and the initial rates of oxygen consumption measured. Conditions: [ferritin] = 4.2 μM, $[O_2]_0$ = 0.28 mM, in 0.1 M NaCl, 75 mM Mops buffer, pH 7.05, 20 °C. Reprinted with permission from Ref. [37].

both ferroxidase site and mineral surface mechanisms are operable under conditions of very high iron loading but the majority of Fe(II) is oxidized on the core surface.

5. Intermediate iron species

The above reaction mechanism for iron oxidation fits available kinetic and structural data quite well. However, several intermediate iron species are observed during the oxidative deposition of iron in ferritin: an Fe(II)–protein complex(es), a monomeric Fe(III)–protein complex, a mixed-valence Fe(II)–Fe(III) dimer, Fe(III)–Fe(III) dimers, Fe(III) clusters of various sizes, and an Fe(III)–tyrosinate complex [32,52–60]. Recent studies using rapid freeze–quench EPR spectroscopy [54] and stopped-flow UV–visible spectroscopy [55–58] have permitted kinetic measurements on a number of these species. How these various species fit into the overall mechanism of iron oxidation and core formation is not completely known. The postulated mechanism given by Eqs. (4)–(7) will undoubtedly have to be modified as additional data become available, especially from rapid kinetics studies.

It seems clear the the protein-catalyzed iron oxidation reaction begins with binding of Fe(II) to the protein. A tightly bound high spin Fe(II) species has been observed in ferritin from *E. coli* bacteria (Ec-FTN) [13]. Fe(II) has also been shown to bind to horse spleen apoferritin [52,60] and holoferritin [60]. Under anaerobic conditions a stoichiometry of 8.0 ± 0.5 is observed in the pH range from 6.0 to 7.5. As the pH is increased to 10.0, up to 80 Fe(II) ions are observed to bind to the apoprotein, while as many as 300 appear to bind to holoferritin. Fe(II) binding is accompanied by electron transfer to the core which, presumably, produces a core-bound Fe(III) ion [60]. Both Fe(III) monomers and dimers whose Mössbauer signals decay with time have been observed after addition of Fe(II) to horse spleen apoferritin, suggesting that these species are intermediates in the process of iron uptake [52]. Isolated Fe(II), isolated Fe(III) and μ-oxo-bridged Fe(III) dimers have been observed in recombinant H chain ferritin and a variety of its variants as well [29,32].

Use of nitric oxide, NO, as a spin probe has also helped determine the presence of both monomeric and dimeric Fe(III) species in bacterioferritin, the dimer presumably being a ferroxidase site species [56,61]. Similar complexes were observed following the anaerobic addition of NO and Fe(II) to horse spleen apoferritin and holoferritin, as well as to apo-HuHF and HuHF variants [62]. Three types of EPR signals were seen in this case: an $S = 1/2$ rhombic species (A-type signal) associated with binding at His 128 and possibly His 118 also, and $S = 1/2$ axial species (B-type signal) associated with binding at Cys 130, and an $S = 3/2$ axial species (C-type signal). The C-type signal is thought to arise from non-specific Fe(II) binding to carboxylate groups on the protein. The C-type spectrum is attributed to a monomeric iron nitrosyl species, and the B-type to an Fe(II) dinitrosyl complex. No information about the nuclearity of the A-type signal was obtained [62]. These studies further emphasize the role of residues in and around the 3-fold channels in iron binding by ferritin.

An intermediate species with a half-life of 50 ms has been detected in the heme-

containing bacterioferritin of *E. coli* by stopped-flow UV–visible spectroscopy [56]. The observed spectral changes in the heme were assumed to be caused by the binding of Fe(II) to non-heme iron binding sites. Maximum absorbance change was observed with the addition of 50 or more Fe(II) to the protein, close to the value of 48 expected for Fe(II) saturation of the dimeric ferroxidase sites on each of the 24 subunits [56]. Monitoring of the absorbance at 340 nm, which is directly associated with non-heme Fe(III) binding, provided evidence for two kinetically distinguishable phases during iron oxidation in Ec-BFR [56]. An exponential increase in absorbance was observed over 20 s when Fe(II) was added to the Ec-BFR in its apo form. The maximum amplitude of the absorbance increase was linear until approximately 50 Fe(II) per protein had been added, at which point the change in absorbance amplitude leveled off, again suggesting saturation of the dimeric ferroxidase sites. When more than 50 Fe(II) per protein were added, a third phase was observed. This more slowly increasing absorbance was attributed to iron oxidation at the surface of the mineralized iron core of the protein [56].

Two types of Fe(II) complexes and two types of Fe(III) dimers as well as Fe(III) monomers and clusters have been observed when solutions of HuHF are monitored by Mössbauer spectroscopy over time following the aerobic addition of Fe(II) [55]. The Fe(III) dimer signals decreased from 0.5 to 10 min and were accompanied by a related increase in Fe(III) monomer which was followed by an eventual increase in Fe(III) clusters in the time period from 0.5 to 30 min. While the data indicate that the monomers are derived directly from the dimers, it is not clear whether both types of dimers yield monomers, or whether an interconversion between types occurs prior to dissociation. Because species formation was monitored only after the first 30 s of oxidation, no information about the initial formation of the dimers is available from this study [55].

Direct observation of early intermediates in the formation of HoSF from apoHoSF was made by Sun and Chasteen using rapid freeze–quench EPR spectroscopy [54]. Previous studies had shown the presence of three EPR signals following the aerobic oxidation of Fe(II) in apoHoSF: a $g' = 4.3$ signal attributed to a monomeric Fe(III)–protein complex [63,64], a $g' = 1.87$ signal from a mixed valence Fe(II)–Fe(III) dimer [59,64,65], and $g = 2.00$ signals attributed to protein radicals [51,59,65]. The formation of the Fe(III)–protein monomer and the mixed-valence Fe(II)–Fe(III) dimer complex was observed in the first second of the quenched reaction together with a heretofore unobserved radical of unknown origin with an EPR spectrum of axial symmetry, $g_{\parallel} = 2.042$ and $g_{\perp} = 2.0033$ [54].

The first signal observed following the initiation of iron oxidation in apoHoSF is that of the Fe(III) monomer at $g' = 4.3$ [54]. It forms at about the same rate that oxygen is consumed and, like the absorbance from the first kinetic phase described by Le Brun et al. [56], is observable within 50 ms, exhibiting an initial burst in intensity which declines rapidly after about 10 s. Most of the EPR-observable Fe(III) produced at the beginning of the iron oxidation reaction is in the monomeric form. The mixed-valence species observed at $g' = 1.87$ is quantitatively derived from the $g' = 4.3$ monomer species in the first second of the reaction. The concentration of this mixed-valence dimer never exceeds a few per cent of the total iron present, which

is too low for observation by Mössbauer spectroscopy. Indeed, when enough dioxygen is present to oxidize all the Fe(II) in the apoferritin solution, the mixed-valence species never accumulates enough to be seen by EPR spectroscopy either. The fact that this species exists only fleetingly and in such low concentrations, however, does not preclude an intermediary role for it in iron core formation [54]. The oxidation of this species could lead to the formation of an Fe(III) dimer, perhaps that described by Le Brun et al. [56] in bacterioferritin or observed by Mössbauer and UV spectroscopy for horse and human ferritins [29,32,52]. The mixed-valence species could also be formed in the 3-fold channels or possibly be a mineral surface species.

The formations of the mixed-valence and radical species do not appear to be related since they exhibit different dependences on Fe(II) concentration [54]. The line shape and g factors of the radical differ from those of the superoxide radical and from those of a previously observed ferritin radical [51]. Also, it does not resemble the EPR spectrum of known tyrosyl radicals in proteins, although tyrosine cannot be ruled out as a possible site for its production. The radical does not appear to be derived from hydroxyl radical damage to the protein either. The fact that the signal decreases with increasing temperature (as a result of rapid spin relaxation) and increases with increasing Fe(II) concentration in the oxidation reaction suggests that the radical is probably associated with a ferrous (or ferric) ion. What role this radical might play in iron oxidation is uncertain, but it may be involved in storing oxidizing equivalents on the protein for subsequent oxidation of Fe(II) [54]. Such redox centers have been observed with horse spleen apoferritin [66].

A rapidly formed Fe(III)–tyrosinate complex first seen in bullfrog H chain ferritin [57,58] and then in HuHF [55] by UV–visible stopped-flow spectroscopy is also a product of iron oxidation, although its precise role in the mechanism of iron oxidation is unclear. Theil and colleagues working with bullfrog ferritin have observed that the absorbance at 550 nm increases rapidly during the first 0.5 s of the reaction [57,58]. However, the protein is unable to re-form the Fe(III)–tyrosinate complex completely until 12 h after the initial reaction [57]. They suggest that regeneration of the Fe(III)–tyrosinate site, postulated to be Tyr 29 (human chain numbering) in bullfrog ferritin, may depend on the completion of other iron reactions following the initial formation of the tyrosinate complex [57].

In HuHF, the putative iron(III)–tyrosinate complex appears within the first 0.5 s of the reaction and decays over approximately 5 s [55]. An increase in absorbance at 360 nm, attributed primarily to Fe(III) dimers, parallels the decrease in absorbance at 550 nm which has been attributed in part to the Fe(III)–tyrosinate complex. In a variant protein of HuHF (Y34F) in which Tyr 34 is changed to a phenylalanine, no absorbance at 550 nm is observed. However, this signal is also absent from spectra of two other variants, E27A and Q141E, where residue 34 is tyrosine. One type of Fe(III) dimer as well as a large number of monomers and some clusters are still produced on aerobic addition of Fe(II) to the Y34F variant, but the rate of Fe(II) oxidation is reduced somewhat compared with the wild type protein [55]. The human protein's ability to function in the absence of Tyr 34 and the apparent time lag between Tyr 34 complex decay and formation of other intermediates suggests that this residue probably does not play a major role in the protein-catalyzed iron

oxidation process. The fact that the second type of Fe(III) dimer is not observed in the protein in which residue 34 has been mutated from tyrosine to phenylalanine and the possibility that the dimer may in some way be dependent on its presence, however, must be considered. Modeling of the human H chain subunit does show that a space exists near the ferroxidase site which could be occupied by an Fe(II) ion bound by both Tyr 34 and Glu 107 [55].

As noted above, several iron species associated with ferritin-catalyzed iron oxidation have been identified, and their order of appearance during the reaction partially established. However, the roles of the various species and their sites of formation on the protein are still uncertain. Additional rapid kinetics studies are needed, especially employing Mössbauer spectroscopy of wild-type and site-directed variant proteins, to relate better the UV–visible and EPR data to the overall mechanism of iron deposition in ferritin.

6. Ferritin cores

Ferritin allows cells to store and use dissolved iron at pH levels that would ordinarily induce Fe(III) precipitation into potentially harmful solid phases [67]. The biomineralization of core formation is complex and incompletely understood. Many studies of model compounds have helped to lay the groundwork for a deeper understanding of this naturally occurring process [68–73]. In general, biomineralization involves three steps: supramolecular preorganization, interfacial molecular recognition, and cellular processing [74,75]. In the supramolecular preorganization process, the organic structure on which mineralization occurs and by which it is controlled is synthesized. In the case of ferritin, this process involves the assembly of a hollow, spherical protein shell from 24 subunits [74,76]. During the interfacial molecular recognition process, nucleation is controlled or directed by the electrostatic, structural and stereochemical interactions at the interface of the organic and inorganic structures [74,75,77]. On the curved inner surface of the ferritin protein shell, only charge and polar interactions are involved. The metal nuclei are kinetically stabilized by the negatively charged glutamate residues. This arrangement results in a lower activation energy of nucleation [74,76]. During the cellular processing stage biomineralization is controlled by cellular activity. For the ferritin molecule this stage involves controlling core size by virtue of cavity size, and, to the extent to which ferritin is able to control the rate of ion exchange within the cavity, control of core composition and crystallinity [74].

Studies of the roles of each of the ferritin subunits in the core formation process and attempts to identify possible nucleation sites on the protein shell's inner surface have involved the use of both site-mutated and native ferritins. A great deal of evidence has been provided for the importance of the L chain subunit in core formation. Large Fe(III) clusters were observed to form following the aerobic addition of Fe(II) to horse spleen apoferritin [26,30,49,78], which consists mostly of L chain subunits (85%). Such cluster formation occurs more slowly in recombinant human H chain ferritins in which the glutamates of the putative nucleation site

(Glu 61, Glu 64, Glu 67) have been changed to alanines [26,78]. Recombinant human L chain ferritin has also been observed to initiate core formation more extensively than an H chain variant with altered ferroxidase sites [49]. In addition to a reduced rate of iron uptake, the H chain variant also produced iron cores with wider particle size distribution than those with unaltered nucleation sites [30].

The increased ability to initiate large cluster formation of the L chain may result from the facts that residue Glu 61 is positioned closer to the cavity face in the L chain subunit than in the H chain, and that residues 57 and 60, which are histidines in the H chain subunit, are glutamates in the L chain subunit. These differences, conferring as they do a higher charge density to the inner surface of the L chain relative to the H chain subunit, may enhance the ability of the L chain to stabilize iron nuclei [49].

Core formation does, however, appear to involve a high degree of cooperativity between the H and L chain subunits. Under acid conditions (pH 5.5–6.0) L chain homopolymers lose their ability to incorporate iron [49,79]. This ability is restored when H chain homopolymers are added to the solution. In addition to demonstrating that iron can exchange between ferritin molecules, this observation also supports the conclusion that core formation depends on both the catalytic oxidation of Fe(II) on the H chain and the stabilizing effect of the L chain on the incipient iron nuclei [49]. This conclusion is further supported by observations of relatively high rates of iron uptake by the L chain rich horse spleen ferritin under acid conditions [27]. Apparently only a few ferroxidase site containing H chain subunits are required to supply the L chain subunits with the necessary Fe(III) for nucleation. Indeed, control of the H:L subunit ratios in ferritin heteropolymers may be one method by which the protein controls core formation in differing biological environments [30].

The size, composition, and structure of the iron core vary widely among the different ferritins. The range extends from relatively large, crystalline cores of low phosphate content in some mammalian ferritins to smaller, more amorphous cores with very high phosphorous to iron ratios which approach 1:1 in certain bacterioferritins [21]. The reasons for these variations are not completely understood. Factors which seem to be involved are iron and phosphate concentrations within the cell and rates of iron deposition at the core. Whether and, if so, how differences in the amino acid sequences in the polypeptide chains of the ferritin subunits affect core characteristics remains unclear.

The role of phosphate in core formation and structure has been addressed in many studies [13,61,80–86]. The decay of the mononuclear Fe(III)–apoferritin complex, as measured by EPR spectroscopy, is accelerated by a factor of 3 when phosphate is added to HoSF following the aerobic addition of Fe(II), presumably by enhancing the protein's ability to convert the mononuclear $g' = 4.3$ Fe(III)–apoferritin complex to EPR-silent polynuclear clusters [86]. Phosphate has also been shown to enhance Fe(II) binding to the mineral core in both HoSF [80] and bacterioferritin from *A. vinelandii* (AVBF) [81]. Addition of phosphate to cores of native AVBF leads to an increase in the protein's ability to bind Fe(II) [81]. This is a result which coincides well with the observation that higher levels of Fe(II) binding are observed in phosphate-rich cores vs. the phosphate poor cores of HoSF. Presumably the phos-

phate catalyzes the internal electron transfer which occurs during Fe(II) oxidation at the core surface [81]. Studies with horse spleen holoferritin demonstrate that reduction of the core results in a release of both phosphate and iron, with a higher percentage of phosphate being released in the earlier stages of reduction than iron [80]. This observation is consistent with the view that the phosphate in the cores of mammalian ferritins is mainly surface bound [80].

The cores from the ferritins of horse spleen, rat liver, and bovine liver have phosphate contents which vary inversely with the iron content [84]. The phosphate associated with these large, highly crystalline cores of high iron content appears to bind to the mineral surface and is easily displaced during iron release or deposition. A significant amount, however, remains associated with the core, an observation which suggests that the addition of iron and phosphate to the core may proceed by separate processes [84]. The cores from ferritins isolated from native pea seed *Pisum sativum* are relatively small (1800 Fe atoms) and amorphous with a relatively low iron to phosphate ratio (Fe:P = 2.83:1). Cores reconstituted in vitro without phosphate are crystalline, however, suggesting that the environment within which the ferritin operates might be more important in determining the core structure than the protein shell itself [83]. The cores of the non-heme-containing ferritins isolated from *E. coli* are either crystalline or amorphous, depending on the amount of phosphate present with high phosphate content cores being more amorphous [13]. The highly disordered cores of *A. vinelandii* bacterioferritin are very high in phosphate content [81]. Overall, cores with higher phosphorous content exhibit lower superparamagnetic blocking temperatures in the Mössbauer spectrum [87].

The absence of phosphate by itself does not ensure a crystalline structure, however. The cores of ferritins from the hemolymph of the chiton *Acanthopleura hirtos* and the limpet *Patella laticostata* are relatively low in phosphate content (1Pi:44Fe for the chiton and 1Pi:36Fe for the limpet). These cores are also low in density and low in crystallinity [82]. The amorphous structure in this case may be related to the rapid rate of iron deposition in forming the core. Both of these organisms have high iron turnover rates and it is suggested that this may lead to the increased core formation rates observed in their ferritins relative to horse spleen ferritin [82]. Similar effects have been observed in other systems as well. An increased rate of iron deposition due to unusually high concentrations of iron has been implicated in the differences observed in the cores of ferritins isolated from the organs of humans with β-thalassemia–hemoglobin E disease [20b]. Ferritins from organs with extremely high iron contents produced smaller, less crystalline cores compared with those isolated from normal organs [20b].

7. Conclusion

Some things seem certain today which were merely conjecture five years ago. The protein has been shown to be an enzyme which catalyzes the oxidation of Fe(II) to Fe(III). Two reaction mechanisms, one protein catalyzed and one involving iron autoxidation at the mineral core, have been described and the reaction stoichiomet-

ries established. Enzyme kinetic parameters for the protein catalyzed oxidation reaction have been determined. Several iron and radical species, some of which may be key intermediates in iron oxidation and core formation, have been identified and their order of appearance during the reaction determined. The presence of a dimeric ferroxidase site on the H chain subunit has now been reasonably well established and several of the ligands necessary for rapid iron oxidation identified. The role of the L chain subunit in stabilizing both incipient iron nuclei and protein structure has also been demonstrated. Questions, however, remain.

It is uncertain which of the identified iron and radical species are essential intermediates in the iron oxidation pathway. Also, it is not clear where on the protein some of the intermediates form or what path within the protein shell iron takes in migrating from the ferroxidase site to the core. The use of recombinant proteins and site-directed variants, high resolution crystallography, and various rapid spectroscopic methods will undoubtedly provide definitive answers to many of these remaining questions about ferritin structure and function.

Acknowledgment

This work was supported by Grant R37 GM20194 from the National Institutes of Health.

References

[1] R.R. Crichton, Inorganic Biochemistry of Iron Metabolism, Ellis Horwood, London, 1991, p. 13.
[2] R.R. Crichton and R.J. Ward, Biochemistry, 31 (1992) 11255.
[3] S.C. Andrews, P. Arosio, W. Bottke, J.F. Briat, M. Von Darl, P.M. Harrison, J.P. Laulhère, S. Levi, S. Lobreaux and S.J. Yewdall, J. Inorg. Biochem., 47 (1992) 161.
[4] P.M. Harrison, S.C. Andrews, P.J. Artymiuk, G.C. Ford, J.R. Guest, J. Hirzmann, D.M. Lawson, J.C. Livingstone, J.M.A. Smith, A. Treffry and S.J. Yewdall, Adv. Inorg. Chem., 36 (1991) 449.
[5] T. Jones, R. Spencer and C. Walsh, Biochemistry, 17 (1978) 4011.
[6] J.G. Joshi and A. Zimmerman, Toxicology, 48 (1988) 21.
[7] E.C. Theil, Annu. Rev. Biochem., 56 (1987) 289.
[8] P.M. Harrison, S.C. Andrews, G.C. Ford, J.M.A. Smith, A. Treffry and J.L. White, in G. Winkelmann, D. van der Helm and J.B. Neilands (eds.), Iron Transport in Microbes, Plants and Animals, VCH, Weinheim, 1987, p. 445.
[9] P.M. Harrison, A. Treffry and T.H. Lilley, J. Inorg. Biochem., 27 (1986) 287.
[10] P.M. Harrison, Biochem. Educ., 14 (1986) 154.
[11] G.C. Ford, P.M. Harrison, D.W. Rice, J.M.A. Smith, A. Treffry, J.L. White and J. Yariv, Philos. Trans. R. Soc. London, Ser. B, 304 (1984) 551.
[12] S.C. Andrews, J.M.A. Smith, S.J. Yewdall, J.R. Guest and P.M. Harrison, FEBS Lett., 293 (1991) 164.
[13] A.J. Hudson, S.C. Andrews, C. Hawkins, J.M. Williams, M. Izuhara, F.C. Meldrum, S. Mann, P.M. Harrison and J.R. Guest, Eur. J. Biochem., 218 (1993) 985.
[14] E.C. Theil, Mol. Biol., 63 (1989) 421.
[15] P. Arosio, T.G. Adelman and J.W. Drysdale, J. Biol. Chem., 253 (1978) 4451.
[16] D.M. Lawson, P.J. Artymiuk, S.J. Yewdall, J.M.A. Smith, J.C. Livingstone, A. Treffry, A. Luzzago,

S. Levi, P. Arosio, G. Cesareni, C.D. Thomas, W.V. Shaw and P.M. Harrison, Nature (London), 349 (1991) 541.
[17] A. Treffry, E.R. Bauminger, D. Hechel, N.W. Hodson, I. Nowik, S.J. Yewdall and P.M. Harrison, Biochem. J., 296 (1993) 721.
[18] (a) D.W. Rice, G.C. Ford, J.L. White, J.M.A. Smith and P.M. Harrison, in E.C. Theil, G.L. Eichhorn and L.G. Marzilli (eds.), Advances in Inorganic Biochemistry, Elsevier Biomedical, New York, 1983, p. 39.
(b) J. Trikha, G.S. Waldo, F.A. Lewandowski, Y. Ha, E.C. Thiel, P.C. Weber and N.M. Allewell, Proteins: Struct., Funct., Genet., 18 (1994) 107.
[19] A. Treffry, P.M. Harrison, M.I. Cleton, W.C. de Bruijn and S. Mann, J. Inorg. Biochem., 31 (1987) 1.
[20] (a) K.M. Towe and W.F. Bradley, J. Colloid Interface Sci., 24 (1967) 384.
(b) T.G. St. Pierre, K.C. Tran, J. Webb, D.J. Macey, B.R. Heywood, N.H. Sparks, V.J. Wade, S. Mann and P. Pootraku, Biol. Met., 4 (1991) 162.
[21] S. Mann, J.V. Bannister and R.J.P. Williams, J. Mol. Biol., 188 (1986) 225.
[22] R.R. Crichton and F. Roman, J. Mol. Catal., 4 (1978) 75.
[23] I.G. Macara, T.G. Hoy and P.M. Harrison, Biochem. J., 126 (1972) 151.
[24] P.D. Hempstead, A.J. Hudson, P.J. Artymiuk, S.C. Andrews, M.J. Banfield, J.R. Guest and P.M. Harrison, FEBS Lett., 350 (1994) 258.
[25] P. Santambrogio, S. Levi, P. Arosio, L. Palagi, G. Vecchio, D.M. Lawson, S.J. Yewdall, P.J. Artymiuk, P.M. Harrison, R. Jappelli and G. Cesareni, J. Biol. Chem., 267 (1992) 14077.
[26] E.R. Bauminger, P.M. Harrison, D. Hechel, I. Nowik and A. Treffry, Nucl. Instrum. Methods Phys. Res. B, 76 (1993) 1.
[27] D.M. Lawson, A. Treffry, P.J. Artymiuk, P.M. Harrison, S.J. Yewdall, A. Luzzago, G. Cesareni, S. Levi and P. Arosio, FEBS Lett., 254 (1989) 207.
[28] S. Sun, P. Arosio, S. Levi and N.D. Chasteen, Biochemistry, 32 (1993) 9362.
[29] A. Treffry, J. Hirzmann, S.J. Yewdall and P.M. Harrison, FEBS Lett., 302 (1992) 108.
[30] V.J. Wade, S. Levi, P. Arosio, A. Treffry, P.M. Harrison and S. Mann, J. Mol. Biol., 221 (1991) 1443.
[31] S. Levi, A. Luzzago, G. Cesareni, A. Cozzi, F. Franceschinelli, A. Albertini and P. Arosio, J. Biol. Chem., 263 (1988) 18086.
[32] E.R. Bauminger, P.M. Harrison, D. Hechel, I. Nowik and A. Treffry, Biochim. Biophys. Acta., 1118 (1991) 48.
[33] S. Levi, A. Luzzago, F. Franceschinelli, P. Santambrogio, G. Cesareni and P. Arosio, Biochem. J., 264 (1989) 381.
[34] J.G. Wardeska, B. Viglione and N.D. Chasteen, J. Biol. Chem., 261 (1986) 6677.
[35] A. Treffry and P.M. Harrison, J. Inorg. Biochem., 21 (1984) 9.
[36] N.D. Chasteen, S. Sun, S. Levi and P. Arosio, in C. Hershko (ed.), Progress in Iron Research, Plenum, New York, 1994, p. 23.
[37] S. Sun and N.D. Chasteen, J. Biol. Chem., 267(35) (1992) 25160.
[38] A. Desideri, S. Stefanini, F. Polizio, R. Petruzelli and E. Chiancone, FEBS Lett., 287 (1991) 10.
[39] P.M. Hanna, N.D. Chasteen, G.A. Rottman and P. Aisen, Biochemistry, 30 (1991) 9210.
[40] G.J. Gerfen, P.M. Hanna, N.D. Chasteen and D.J. Singel, J. Am. Chem. Soc., 113 (1991) 9513.
[41] R.F. Boyer, S.M. Generous, T.J. Nieuwenhuis and R.A. Ettinger, Biotechnol. Appl. Biochem., 12 (1990) 79.
[42] S. Stefanini, A. Desideri, P. Vecchini, T. Drakenberg and E. Chiancone, Biochemistry, 28 (1989) 378.
[43] N.D. Chasteen, E.M. Lord, H.J. Thompson and J.K. Grady, Biochim. Biophys. Acta, 884 (1986) 84.
[44] J.S. Rohrer, M.S. Joo, E. Dartyge, D.E. Sayers, A. Fontaine and E.C. Theil, J. Biol. Chem., 262 (1987) 13385.
[45] G. Melino, S. Stefanini, E. Chiancone and E. Antonini, FEBS Lett., 86 (1978) 136.
[46] A. Treffry, J.M. Sowerby and P.M. Harrison, FEBS Lett., 95 (1978) 221.
[47] D.E. Mayer, J.S. Rohrer, D.A. Schoeller and D.C. Harris, Biochemistry, 22 (1983) 876.
[48] B. Xu and N.D. Chasteen, J. Biol Chem., 266 (1991) 19965.
[49] S. Levi, S.J. Yewdall, P.M. Harrison, P. Santambrogio, A. Cozzi, E. Rovida, A. Albertini and P. Arosio, Biochem. J., 288 (1992) 591.

[50] P. Santambrogio, S. Levi, A. Cozzi, E. Rovida, A. Albertini and P. Arosio, J. Biol. Chem., 268 (1993) 12744.
[51] J.K. Grady, Y. Chen, N.D. Chasteen and D.C. Harris, J. Biol. Chem., 264 (1989) 20224.
[52] E.R. Bauminger, P.M. Harrison, I. Nowik and A. Treffry, Biochemistry, 28 (1989) 5486.
[53] E.R. Bauminger, P.M. Harrison, D. Hechel, I. Nowik and A. Treffry, Hyperfine Interact., 71 (1992) 1287.
[54] S. Sun and N.D. Chasteen, Biochemistry, 33(50) (1994) 15095.
[55] E.R. Bauminger, P.M. Harrison, D. Hechel, N.W. Hodson, I. Nowik, A. Treffry and S.J. Yewdall, Biochem. J., 296 (1993) 709.
[56] N.E. Le Brun, M.T. Wilson, S.C. Andrews, J.R. Guest, P.M. Harrison, A.J. Thomson and G.R. Moore, FEBS Lett., 333 (1993) 197.
[57] G.S. Waldo and E.C. Theil, Biochemistry, 32 (1993) 13262.
[58] G.S. Waldo, J. Ling, J. Sanders-Loehr and E.C. Theil, Science, 259 (1993) 796.
[59] P.M. Hanna, Y. Chen and N.D. Chasteen, J. Biol. Chem., 266 (1991) 886.
[60] D. Jacobs, G.D. Watt, R.B. Frankel and G.C. Papaefthymiou, Biochemistry, 28 (1989) 9216.
[61] N.F. Le Brun, M.R. Cheesman, A.J. Thomson, G.R. Moore, S.C. Andrews, J.R. Guest and P.M. Harrison, FEBS Lett., 323 (1993) 261.
[62] M. Lee, P. Arosio, A. Cozzi and N.D. Chasteen, Biochemistry, 33 (1994) 3679.
[63] N.D. Chasteen and E.C. Theil, J. Biol. Chem., 257 (1982) 7672.
[64] L.P. Rosenberg and N.D. Chasteen, in P. Saltman and J. Hegenauer (eds.), The Biochemistry and Physiology of Iron, Elsevier Biomedical, New York, 1982, p. 405.
[65] N.D. Chasteen, B.C. Antanaitis and P. Aisen, J. Biol. Chem., 260 (1985) 2926.
[66] R.K. Watt, R.B. Frankel and G.D. Watt, Biochemistry, 31 (1992) 9673.
[67] S. Mann and C.C. Perry, Adv. Inorg. Chem., 36 (1991) 137.
[68] K.L. Taft, G.C. Papaefthymiou and S.J. Lippard, Science, 259 (1993) 1302.
[69] K.S. Hagen, Angew. Chem., Int. Edn. Engl., 31 (1992) 1010.
[70] S.M. Gorun, G.C. Papaefthymiou, R.B. Frankel and S.J. Lippard, J. Am. Chem. Soc., 109 (1987) 3337.
[71] Q.T. Islam, D.E. Sayers, S.M. Gorun and E.C. Theil, J. Inorg. Biochem., 36 (1989) 51.
[72] B.P. Murch, P.D. Boyle and L. Que, Jr., J. Am. Chem. Soc., 107 (1985) 6728.
[73] A.N. Mansour, C. Thompson, E.C. Theil, N.D. Chasteen and D.E. Sayers, J. Biol. Chem., 260 (1985) 7975.
[74] S. Mann, Nature (London), 365 (1993) 499.
[75] S. Mann, Nature (London), 349 (1991) 285.
[76] S. Mann, D.D. Archibald, J.M. Didymus, T. Douglas, B.R. Heywood, F.C. Meldrum and N.J. Reeves, Science, 261 (1993) 1286.
[77] S. Mann, J. Chem. Soc., Dalton Trans., 1 (1993) 1.
[78] E.R. Bauminger, P.M. Harrison, D. Hechel, I. Nowik and A. Treffry, Proc. R. Soc. B, 244 (1991) 211.
[79] S. Levi, P. Santambrogio, A. Cozzi, E. Rovida, B. Corsi, E. Tamborini, S. Spada, A. Albertini and P. Arosio, J. Mol. Biol., 238 (1994) 649.
[80] H. Heqing, R.K. Watt, R.B. Frankel and G.D. Watt, Biochemistry, 32 (1993) 1681.
[81] G.D. Watt, R.B. Frankel, D. Jacobs, H. Huang and G.C. Papaefthymiou, Biochemistry, 31 (1992) 5672.
[82] T.G. St. Pierre, K.S. Kim, J. Webb, S. Mann and D.P.E. Dickson, Inorg. Chem., 29 (1990) 1870.
[83] V.J. Wade, A. Treffry, J.P. Laulhère, E.R. Bauminger, M.I. Cleton, S. Mann, J.F. Briat and P.M. Harrison, Biochim. Biophys. Acta, 1161 (1993) 91.
[84] D. Desilva, J.H. Guo and S.D. Aust, Arch. Biochem. Biophys., 303 (1993) 451.
[85] J.S. Rohrer, Q.T. Islam, G.D. Watt, D.E. Sayers and E.C. Theil, Biochemistry, 29 (1990) 259.
[86] Y.G. Cheng and N.D. Chasteen, Biochemistry, 30 (1991) 2947.
[87] T.G. St. Pierre, S.H. Bell, D.P.E. Dickson, S. Mann, J. Webb, G.R. Moore and R.J.P. Williams, Biochim. Biophys. Acta, 870 (1986) 127.